A Single-Crystal Silicon Symmetrical and Decoupled MEMS Gyroscope on an Insulating Substrate

Said Emre Alper and Tayfun Akin, *Member, IEEE*

***Abstract*—This paper presents a single-crystal silicon symmetrical and decoupled (SYMDEC) gyroscope implemented using the dissolved wafer microelectromechanical systems (MEMS) process on an insulating substrate. The symmetric structure allows matched resonant frequencies for the drive and sense vibration modes for high-rate sensitivity and low temperature-dependent drift, while the decoupled drive and sense modes prevents unstable operation due to mechanical coupling, achieving low bias-drift. The 12–15-μm-thick single-crystal silicon structural layer with an aspect ratio of about 10 using DRIE patterning provides a high sense capacitance of 130 fF, while the insulating substrate provides a low parasitic capacitance of only 20 fF. A capacitive interface circuit fabricated in a 0.8-μm CMOS process and having a sensitivity of 33 mV/fF is hybrid connected to the gyroscope. Drive and sense mode resonance frequencies of the gyroscope are measured to be 40.65 and 41.25 kHz, respectively, and their measured variations with temperature are $+18.28$ Hz/ °C and $+18.32$ Hz/ °C, respectively, in -40 °C to $+85$ °C temperature range. Initial tests show a rate resolution around 0.56 deg/s with slightly mismatched modes, which reveal that the gyroscope can provide a rate resolution of 0.030 deg/s in 50-Hz bandwidth at atmospheric pressure and 0.017 deg/s in 50-Hz bandwidth at vacuum operation with matched modes. [1195]**

***Index Terms*—Capacitive interface, decoupled gyroscope, dissolved wafer process, MEMS gyroscope.**

I. Introduction

MICROELECTROMECHANICAL systems (MEMS) gyroscopes have attracted a lot of attention in the past decade for applications requiring low-cost and compact size gyroscopes with moderate performance, such as automotive safety systems, camera stabilization, and inertial mice. There is also a need for high-performance MEMS gyroscopes for tactical-grade applications, and there is a continuing worldwide effort to implement tactical-grade gyroscopes. The need for tactical-grade MEMS gyroscopes requires challenging mechanical and electrical design tradeoffs. The tradeoffs to reach ultimate performance are well defined but there are also practical problems related to the fabrication limitations, gain/bandwidth considerations, as well as some indeterministic parameters such as temperature-dependent drift and misaligned vibration modes.

Most of the MEMS gyroscopes are based on the Coriolis coupling principle [1]. In these gyroscopes, it is advantageous to match the resonant frequencies of the drive and sense modes to improve the rate sensitivity by the mechanical quality factor of the sense mode [1]. This can be easily achieved by having symmetric suspensions for both modes; however, structures having symmetric suspensions are usually subject to unstable operation and high bias drift due to mechanical coupling between the drive and sense modes [2]. Therefore, the two modes should mechanically be decoupled from each other. There are decoupled gyroscopes to lower the bias drift, but their suspensions are not symmetric, and therefore, they are subject to temperature dependent drift [3]. The symmetrical and decoupled gyroscope structures provide both matched frequencies and decoupled-operation with a dedicated mechanical structure [4]–[9]. We have demonstrated our first symmetric and decoupled (SYMDEC) gyroscope through a polysilicon surface micromachining process (MUMPS) of Cronos Inc., but this implementation provides a limited rate resolution of 1.6 deg/s, with matched drive and sense modes, due to the thin structural layer of 2 μm and high parasitic capacitance of 3 pF due to the conductive silicon substrate [4]. We then reported the second generation SYMDEC gyroscopes that are implemented using an electroformed nickel structural layer on an insulating substrate that decreases the parasitic signal coupling by two orders of magnitude [5]–[7]. Even though we are able to achieve structural layer thicknesses up to 16 μm using standard thick photoresists, the sensor capacitances are limited to less than 65 fF due to low aspect ratios (up to 6) of these photoresists. Even though, special thick photoresists, such as SU-8, can be used to achieve higher aspect ratios, the use of electroplating to implement vibratory gyroscopes is not desired due to the long term reliability of the electroplated structures. This paper reports the development of the third generation SYMDEC gyroscope using single-crystal silicon structural layer on glass substrate [9]. This gyroscope has 12–15-μm-thick structural layer defined by deep boron diffusion [10] and an aspect ratio of about 10 using DRIE patterning, providing a higher sense capacitance of 130 fF. The gyroscope also has a low parasitic capacitance of only 20 fF, as it is implemented on a glass substrate using the dissolved wafer process.

II. Gyroscope Structure

Fig. 1 shows the perspective view of the symmetric and decoupled gyroscope structure. The gyroscope is continuously driven into oscillation along the drive mode (x axis) at the drive mode mechanical resonance frequency by electrostatic excitation applied between the movable and stationary drive fingers. When an external angular rotation is applied about the sensitive axis (z axis), the gyroscope gives an output response

Manuscript received November 10, 2003; revised December 6, 2004. This work was supported by The Scientific and Technical Research Council of Turkey (TUBITAK-EEEAG 100E020) and by State Planning Organization. Subject Editor G. K. Fedder.

The authors are with the Department of Electrical and Electronics Engineering, Middle East Technical University, Ankara, Turkey (e-mail: tayfun-akin@metu.edu.tr).

Digital Object Identifier 10.1109/JMEMS.2005.845400

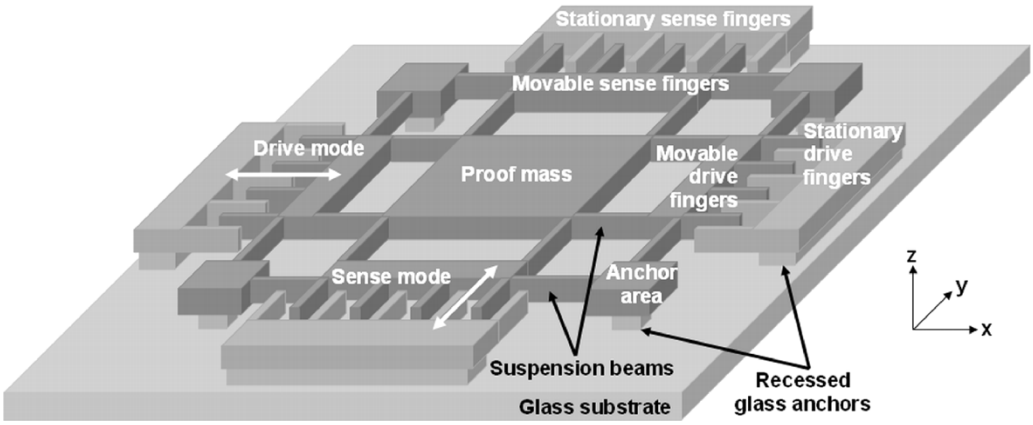

Fig. 1. Three-dimensional structure of the symmetrical and decoupled microgyroscope.

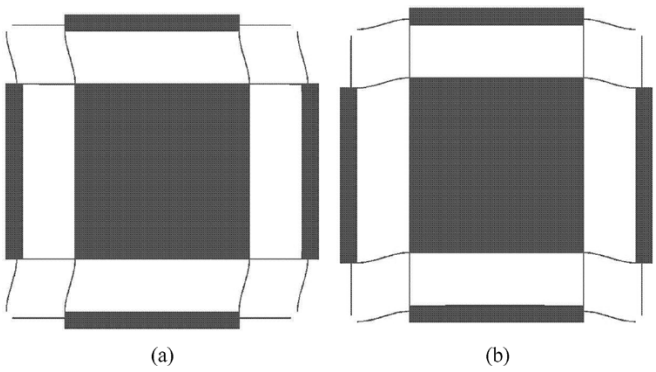

Fig. 2. CoventorWare finite element modal simulations showing the (a) drive and (b) sense modes of the gyroscope matched at 42 025 Hz.

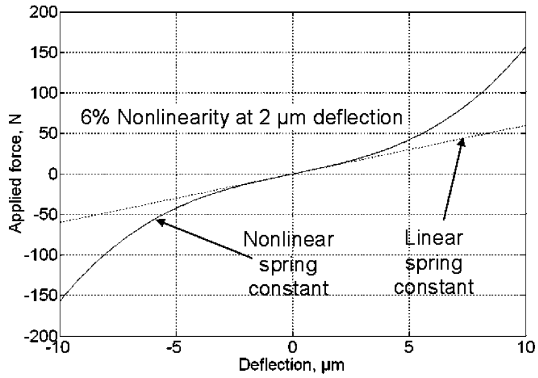

Fig. 3. Spring constant simulations with CoventorWare showing that the gyro must be excited to vibration amplitude less than 2 μm to keep spring nonlinearity below 6%.

along the sense mode (y axis) due to the Coriolis force, whose frequency is identical to the drive mode resonance frequency. If the mechanical resonant frequencies of the drive and sense modes are closely matched, then the sense mode response is maximized. This response is then detected using capacitive readout techniques.

The drive and sense mode resonance frequencies can be easily matched by symmetric design of the suspension beams along the two modes. However, symmetric suspension beams usually result in higher drift rate due to undesired mechanical coupling from the drive mode to the sense mode. This problem is prevented in the proposed gyroscope by placing the anchors at the outermost corners and connecting them to the movable drive and sense electrodes in such a way that the vibration of the drive electrodes does not disturb the sense electrodes. As a result, the SYMDEC gyroscope achieves mechanical decoupling while preserving the advantages of the symmetric structure, i.e., the effect of drift in mode matching is minimized without losing sensitivity.

The sensitivity of the gyroscope is further improved by minimizing the parasitic electrical signal coupling through the substrate with the use of Pyrex glass as the substrate material. Since the thermal expansion coefficient of the Pyrex glass and single-crystal silicon are closely matched for temperatures up to 400 °C, the gyroscope has a low temperature dependent drift over a wide range of ambient temperatures.

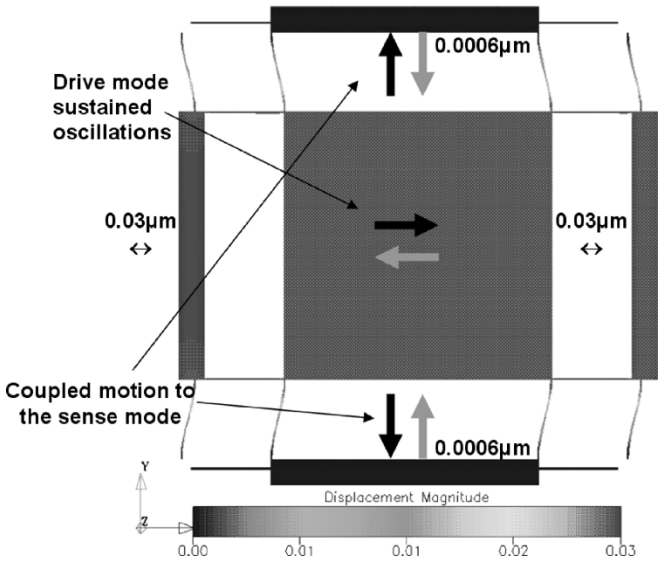

Fig. 4. FEM simulations showing the mechanical coupling between the modes is less than 2%, as a 0.03-μm drive mode vibration amplitude results in a 0.0006-μm common-mode coupling signal to the sense mode.

III. Design and Simulations

Finite-element simulations are performed with CoventorWare to analyze the effects of various nonlinearities such as

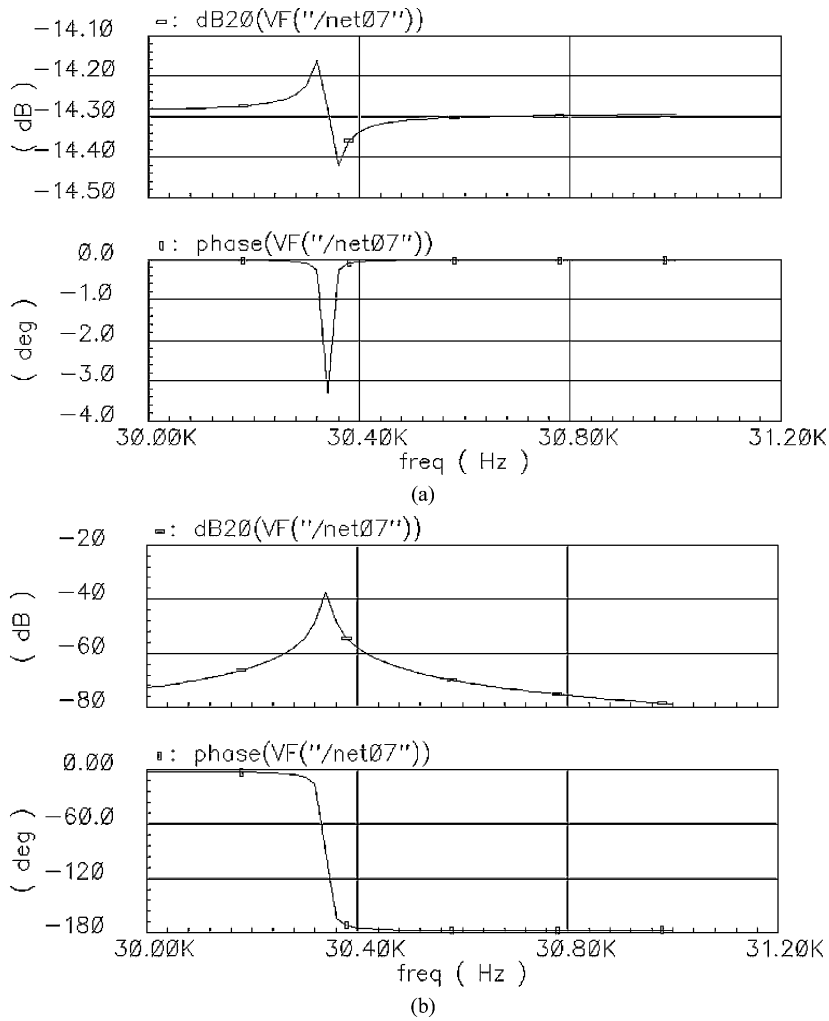

Fig. 5. The simulations performed by SPICE on the lumped element model of the gyroscope, showing the effect of parasitic capacitances when (a) conducting and (b) insulating substrates are used.

spring softening, electrostatic fringe-field effects, and mechanical coupling. Using the results of these FEM simulations, lumped analytical models are constructed in SPICE and SIMULINK to tune the electromechanical parameters of the gyroscope to the desired values by including the aforementioned nonlinear effects.

Fig. 2 shows the finite element simulations performed using CoventorWare software, in which the resonance frequencies of the drive and sense vibration modes are determined to be matched at 42 025 Hz. The three-dimensional (3-D) solid model does not contain the etch holes on the proof mass and the comb fingers for simplified meshing, however, the simulations take into account these effects by using an effective equivalent mass density. In addition, the residual stress of the boron-doped silicon structural layer is also accounted in the simulations. As a result of this accurate model, the simulated resonance frequencies are determined to be very close to the measured drive and sense resonance frequencies.

Fig. 3 shows the simulated spring-constants for the drive and sense modes of the designed gyroscope. This simulation shows that the gyroscope drive mode vibration amplitude should be limited to below 2 μm to keep the spring-constant nonlinearity smaller than 6%.

Fig. 4 presents the FEM simulation result showing that the mechanical coupling from the drive mode to the sense mode is less than 2% of the drive mode vibration amplitude, as a 0.03-μm drive mode vibration amplitude results in a 0.0006-μm common-mode coupling signal to the sense mode. Since this small coupling affects the both sides of the sense electrodes as a common-mode signal, it is suppressed by using a differential readout scheme. In addition, it should be noted that the frequency of the coupling signal is twice that of the drive mode, since the sense mode electrode moves twice when the drive mode electrode moves once, due to the mechanical structure of the gyroscope. This high-frequency coupling signal is then further suppressed through the low-pass filters of the readout electronics after demodulating the output signal of the gyroscope by drive-mode resonance-frequency, resulting in very low quadrature error signal. In summary, this simulation verifies that the structure proposed in this paper provides both symmetrical and decoupled operation.

Fig. 5 shows the simulations performed on the lumped element model of the gyroscope constructed in SPICE, demonstrating that the electrical cross-coupling is reduced by more than two orders of magnitude if the device is fabricated on an insulating substrate instead of a conductive silicon substrate.

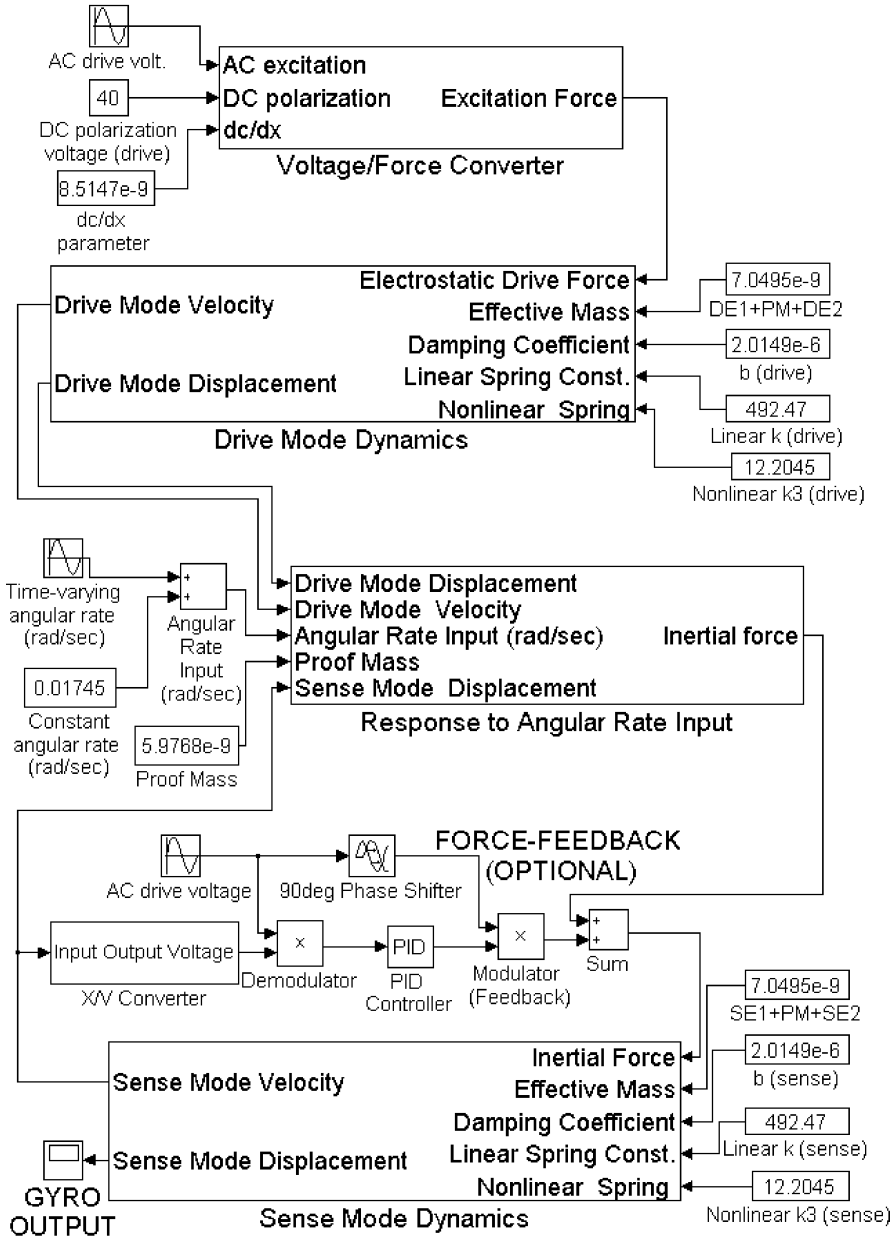

Fig. 6. Behavioral model of the designed gyroscope constructed in SIMULINK.

This can be understood by observing the height of the resonance peak, i.e., the difference between the peak signal level at resonance and the flat-band signal level out of resonance. The height of the resonance peak is only a fraction of a dB for conducting substrates, whereas it reaches to more than 30 dB for insulating substrates. The resonance characteristics obtained for conducting substrates include the mechanical resonance characteristics as well as electrical antiresonance characteristics due to the combinational effects of parasitic stray capacitances and substrate conductance. Insulating substrates, on the other hand, highly suppress electrical cross coupling due to minimized parasitic capacitance and substrate conductance, and, therefore, provide the bare mechanical resonance characteristics of the sensor without showing an electrical antiresonance peak. As a result, the use of insulating glass substrate improves the signal-to-noise ratio (SNR) of the gyroscope by a factor more than 100.

Fig. 6 shows the behavioral model of the gyroscope constructed in SIMULINK. This model includes some of the second-order effects like spring softening, electrostatic force nonlinearity, and viscous air damping to accurately estimate the resonance frequencies, angular rate sensitivity, start-up time, bandwidth, and electrical cross-coupling parameters of the gyroscope prior to fabrication. The angular rate resolution of the gyroscope is simulated to be 0.45 deg/s in a bandwidth of 50 Hz using the constructed model when the drive and sense mode frequencies are slightly mismatched (by 600 Hz). In this simulation, the drive mode vibration amplitude is limited to 2 μm, the dc polarization voltage applied to the proof mass is set to 40 V, the input capacitance of the capacitive interface circuit is taken as 50 fF, and the output noise floor of the overall system is set as 1 $\mu\mathrm{V}/\mathrm{Hz}^{1/2}$. When the frequencies of the two modes are accurately matched and the gyro is operated at

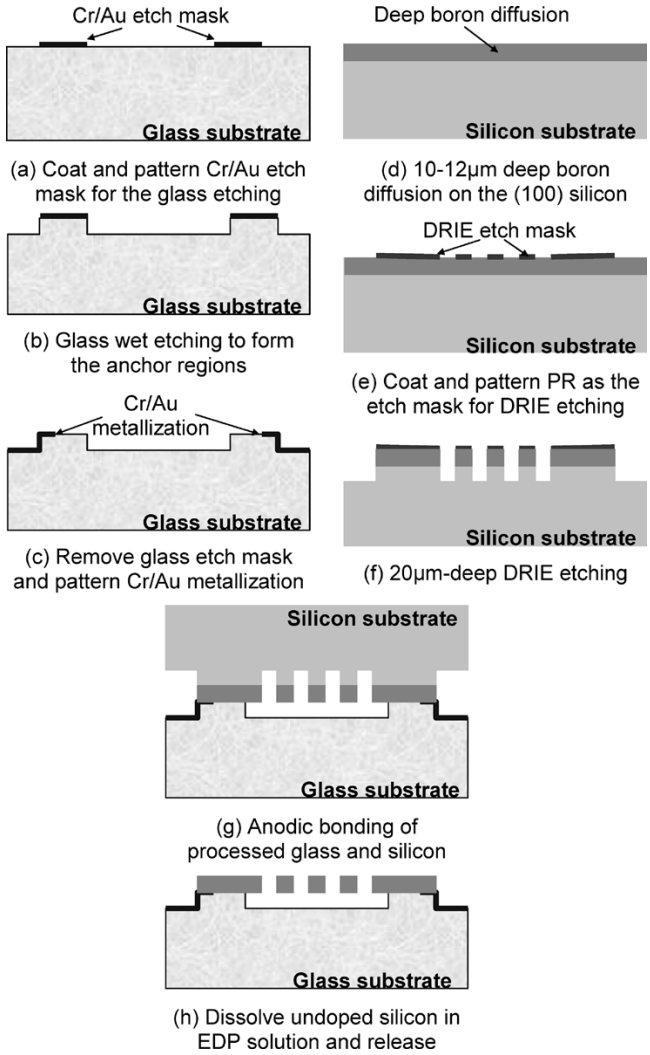

Fig. 7. Fabrication process, which is based on the dissolved wafer process.

atmospheric pressure with a sense mode quality factor of 800, the behavioral model estimates a rate resolution of 0.03 deg/s for the gyroscope in 50-Hz bandwidth.

IV. Fabrication Process

The fabrication process is a very simple three mask process, and it is based on the dissolved wafer process [10] combined with the deep reactive ion etching (DRIE). Fig. 7 shows the process steps. First, a deep-boron diffusion of 12–15 μm is performed on the front side of a (100) silicon wafer to a high doping density around 10^{20} atoms/cm^{-3}. Then, a 20–25-μm DRIE etch is performed from the boron doped front side of the silicon wafer to form the gyroscope patterns. The silicon wafer is then flipped and anodically bonded to a recessed Pyrex glass wafer from the anchor regions. Finally, the undoped silicon wafer is completely dissolved in an EDP solution, leaving the boron-doped single-crystal silicon structures on the glass substrate and forming the gyroscopes.

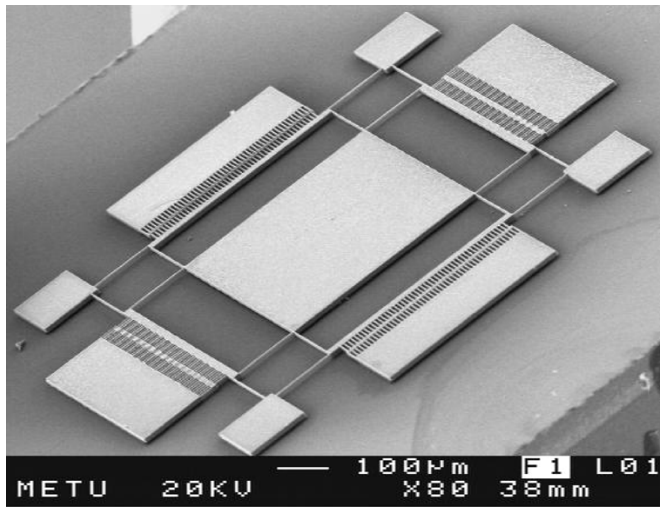

Fig. 8. SEM picture of the fabricated microgyroscope. The gyroscope occupies an area of 1 mm × 1 mm.

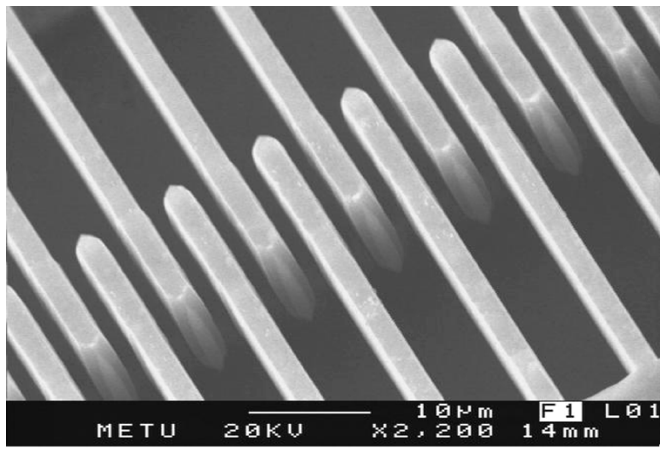

(a)

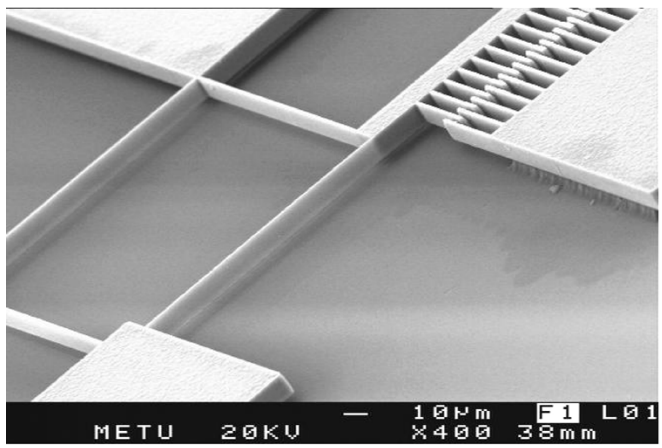

(b)

Fig. 9. Closer SEM picture of the high-aspect ratio comb fingers with 12 μm height and 1.5 μm spacing.

V. Implementation and Test Results

Figs. 8 and 9 show the SEM pictures of one of the fabricated gyroscopes. The overall size of the gyroscope is approximately 1 mm × 1 mm. The height of the structural layer of the gyroscope is measured as 12 μm, whereas the electrostatic gap between the fabricated comb fingers is 1.5 μm, slightly larger than

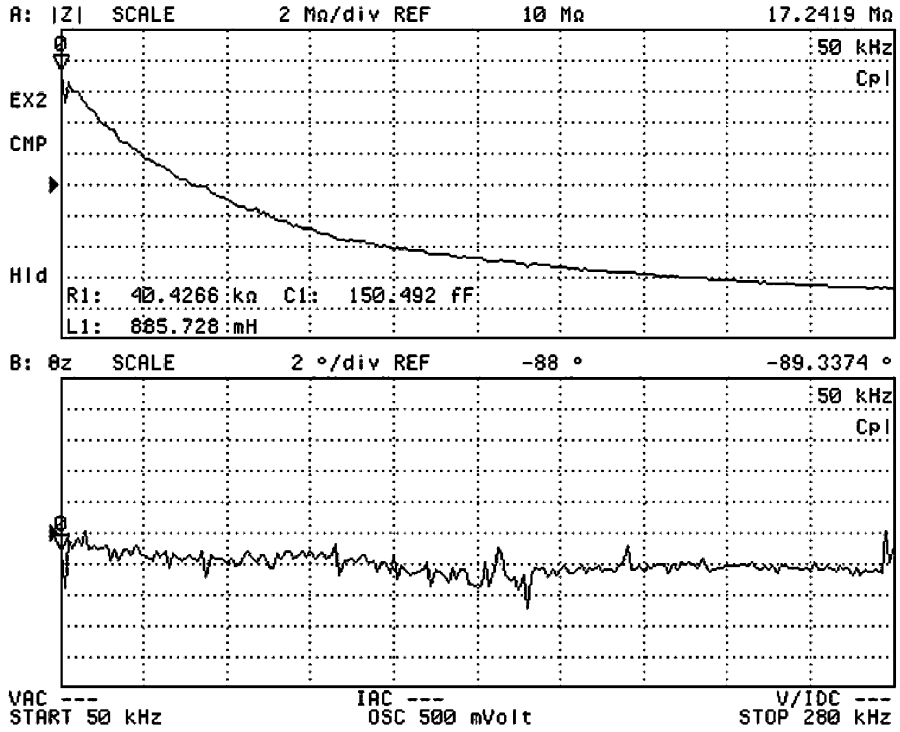

Fig. 10. Capacitance measurements for the fabricated gyroscope, showing a total capacitance of 150 fF, which includes the sensor capacitance and the parasitic capacitance.

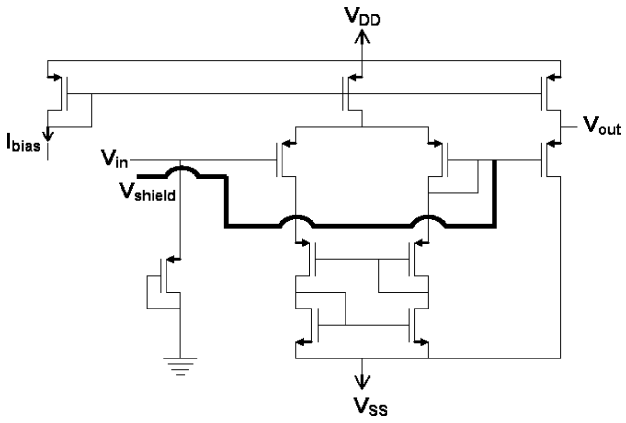

Fig. 11. Schematic view of the unity-gain buffer type capacitive interface circuit with a bootstrap shield to minimize parasitic capacitances.

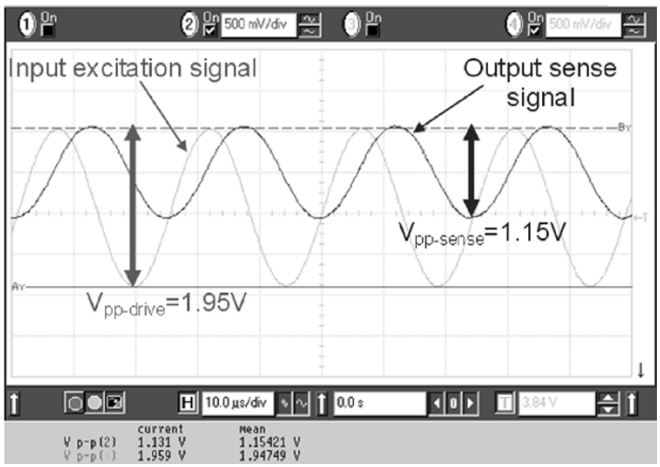

Fig. 12. The input excitation signal for drive mode resonance and the corresponding output signal picked by the interface circuit. The measurements correspond to an input capacitance lower than 50 fF (limited by wirebonding) and sensitivity of 34 mV/fF for the fabricated interface circuit.

the mask opening of 1 μm due to mask undercut of the DRIE. The aspect ratio of the currently fabricated gyroscope is close to 10, but can be increased further by reducing the DRIE mask undercut. The current aspect ratio allows the gyroscope sensor capacitances to be over 100 fF. The flexures and the proof mass are suspended 5 μm over the substrate reducing the air damping significantly for operation at atmospheric pressure.

The parasitic and sensor capacitances of the gyroscope are measured by the HP4294A impedance analyzer. Fig. 10 shows the results of these measurements, where the sensor capacitance and the parasitic capacitance are measured to be 130 and 20 fF, respectively. These values closely match with the calculation and simulation results. The sensor capacitance is about 2–10 times larger compared to the other SYMDEC gyroscopes fabricated by conventional surface micromachining processes, where the aspect ratio is smaller [4]–[7]. This high capacitance is a result of high-aspect ratio DRIE patterning of the comb fingers, whereas the low parasitic capacitance is due to the insulating glass substrate. The small parasitic capacitance also suppresses the direct electrical feedthrough from the drive mode to the sense mode, increasing the SNR of the gyroscope.

The fabricated gyroscopes are hybrid connected to a capacitive interface circuit fabricated in a 0.8 μm CMOS process. Fig. 11 shows the schematic view of the interface circuit that uses a unity-gain buffer structure [11] to measure small capacitive deflections. The input of the buffer circuit is biased with

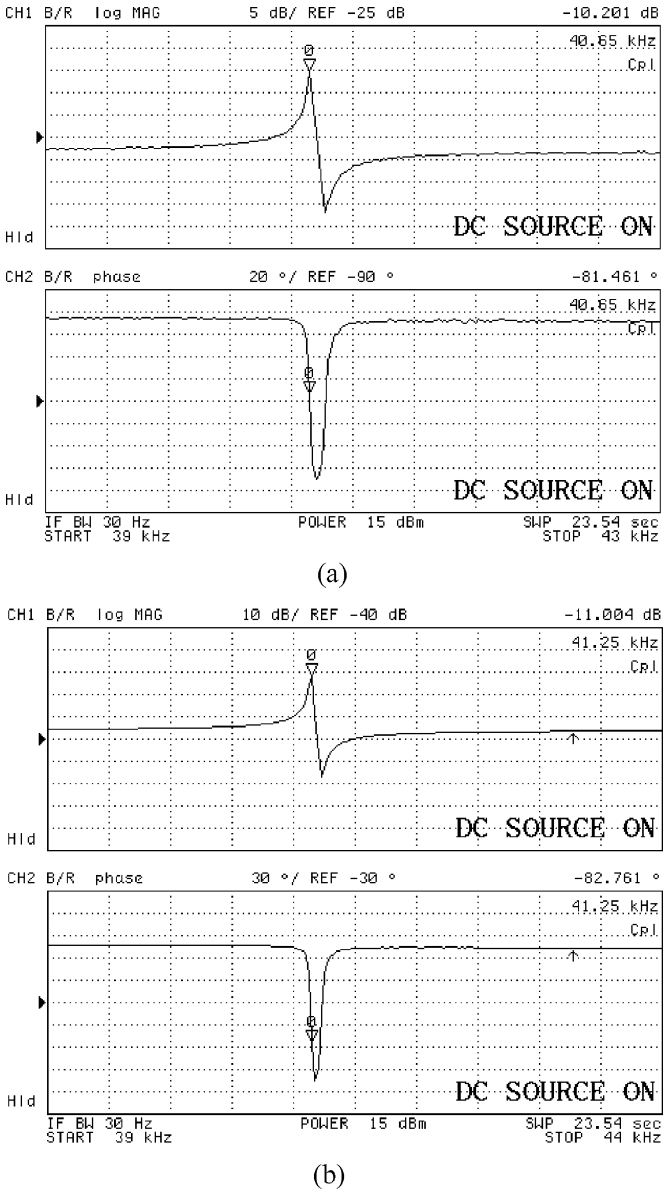

Fig. 13. Measured (a) drive and (b) sense mode resonance frequencies of the gyroscope hybrid connected to the capacitive interface circuit. The drive and sense mode resonance frequencies are measured as 40 650 and 41 250 Hz, respectively.

a minimum-size PMOS transistor operating in sub threshold region to keep the input capacitance of the interface circuit small. In addition, a metal bootstrap shield is placed underneath the input metallization of the interface circuit, which effectively suppresses any parasitic capacitances to the substrate of the CMOS chip. As a result, the input capacitance of the capacitive interface circuit is lowered to about 50 fF, limited by the hybrid wire-bonding capacitance. Fig. 12 shows the input excitation signal for the drive mode resonance and the corresponding output signal picked by the interface circuit. The peak-to-peak value of the drive mode excitation signal is 1.95 V, while the peak-to-peak value of the measured signal at the drive mode output is 1.15 V, with a 150-V dc polarization voltage applied to the gyro proof mass. At this condition, the vibration amplitude is measured as 3.9 μm, corresponding to

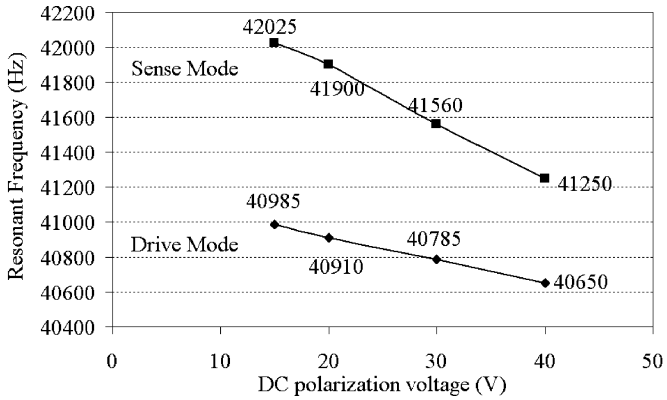

Fig. 14. Measured trends of drive and sense mode resonance frequencies when dc bias voltages up to 40 V is applied to the drive and sense electrodes separately.

a capacitance change of 34 fF at the gyroscope output. By dividing the interface circuit output signal by this capacitance change, the sensitivity of the fabricated interface circuit is determined as 34 mV/fF. It should be noted here that the large vibration amplitude of 3.9 μm was selected only during the sensitivity measurements of the fabricated capacitive interface circuit in order to maximize the amount of capacitance change at the gyroscope output. Although such a large deflection results in nonlinear mechanical behavior, it does not affect the capacitance sensitivity measurements of the interface circuit. In normal operation, the vibration amplitude is kept below 2 μm reduce nonlinearity due to the spring stiffening effects.

Fig. 13 shows the drive and sense mode resonance frequencies which are measured as 40 650 and 41 250 Hz, respectively, by using the HP4395A network analyzer and a 40-V dc polarization voltage. The mismatch between the two frequencies is only 600 Hz, and it is believed to be mainly due to a thin-layer of undoped silicon that remained on top of the p^{++} doped proof mass (as seen in Fig. 9), causing a nonuniform mass distribution. This nonuniform mass distribution can be nulled with the use of electrostatic springs created with appropriately located balance electrodes, which is under consideration for future designs. Another method to compensate the non uniform mass distribution and the resulting resonance frequency mismatch is to apply different dc bias voltages to the drive and sense electrodes separately, by keeping the proof mass at ground potential. A last point about the measurements in Fig. 13 is that the antiresonance peaks are apparent in the measured resonance characteristics although the substrate of the gyroscope is insulating, which is due to the high capacitive feedthrough of the external measurement setup. Fig. 14 shows the measured trends of drive and sense mode resonance frequencies when dc bias voltages up to 40 V is applied to the drive and sense electrodes separately. The frequency mismatch can be decreased down to 265 Hz by applying 15-V dc bias to the drive electrode and 40-V dc bias to the sense electrode. Applying dc bias voltages higher than the multiples of 40 V may cause pull-in of the proof mass to the electrodes or substrate. However, note that keeping the drive mode dc bias at 15 V would also decrease the drive mode vibration amplitude as well as the rate sensitivity. Therefore, a constant dc bias voltage of 40 V is applied to the proof mass throughout the tests. Fig. 15

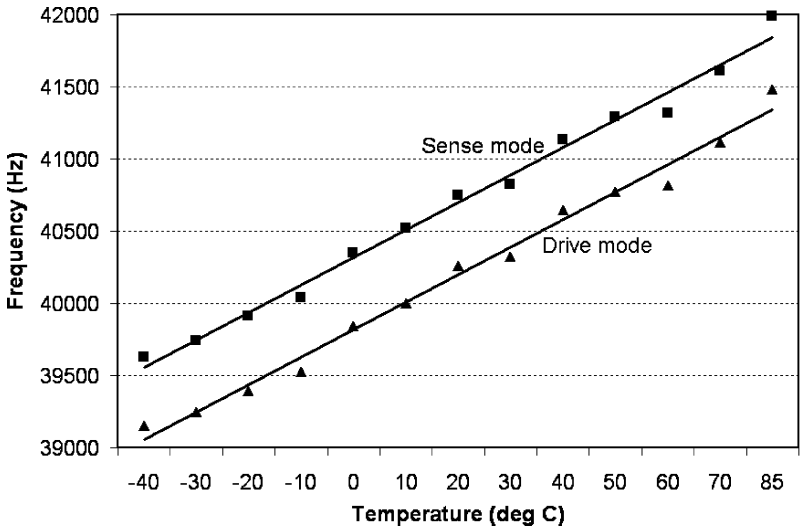

Fig. 15. Measured drive and sense mode resonance frequency shift for different ambient temperatures. The resonance frequency shift is less than $\pm 3\%$ in the measured temperature range of -40 °C to $+85$ °C, whereas the mismatch between the resonance frequencies is much more robust.

shows measured drive and sense mode resonance frequency shift for different ambient temperatures. The measured drive and sense resonance frequency shifts with temperature are $+18.28$ Hz/°C and $+18.32$ Hz/°C, respectively, in -40 °C to $+85$ °C temperature range. This measurement proves the advantage of having a symmetrical design. Once the small mismatch between the modes is achieved with electrostatic tuning, the matching of the modes will be preserved, which is very important to substantially reduce the temperature drift of the gyroscope.

The gyroscope is excited to 2 μm vibration amplitude with 4 Vp-p ac signal at the resonance frequencies of both modes while applying a dc polarization signal of 40 V. Optical investigation of the resonance bandwidth with the help of an optical setup yields quality factors of above 500 at atmospheric pressure. These large quality factors are due to the 5 μm spacing between the substrate and the proof mass, the optically measured quality factors agree with the quality factors extracted from the network analyzer measurements. The quality factors measured by the network analyzer are slightly lower than the simulated quality factors, which is due to the fact that the FEM simulations take into account only the slide film damping and neglect the squeeze film effects.

The sense mode response amplitude of a micromachined gyroscope with matched drive and sense mode frequencies is simply expressed by the following [12]

$$Y(\omega) = \frac{2 \cdot \Omega_0 \cdot X_0 \cdot Q_{\text{sense}}}{j \cdot \omega_{\text{drive}}} \tag{1}$$

where Ω_0 is the applied angular rate input, X_0 is the drive mode vibration amplitude, Q_{sense} is the mechanical quality factor of the sense mode, and ω_{drive} is the drive mode resonance frequency in rad/s. Obviously, the sense mode response of such a gyroscope is highly improved if the gyroscope is operated at vacuum to provide a Q_{sense} on the order of a few thousand that can be achieved with the single-crystal silicon structural layer. However, for a gyroscope with slightly mismatched resonance

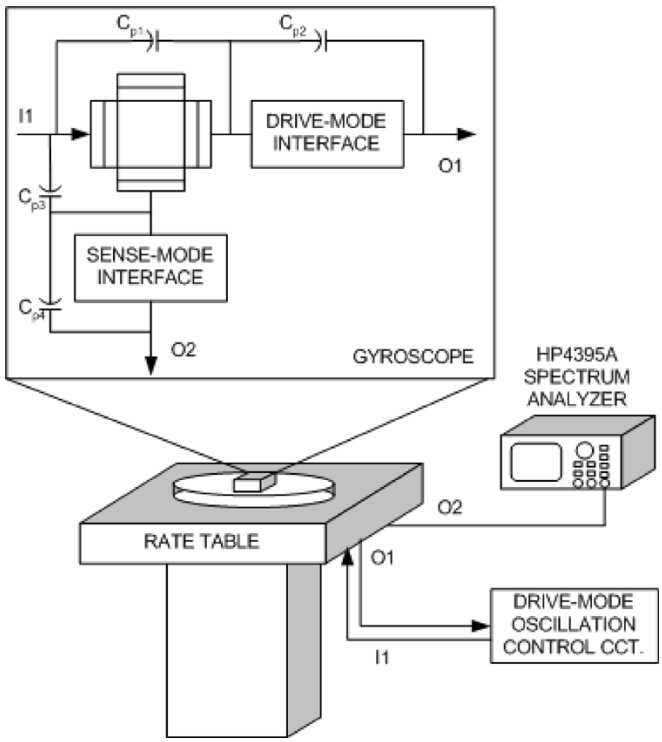

Fig. 16. Schematic of the test setup for measuring the angular rate response of the gyroscope.

frequencies for the drive and sense modes, the sense mode response amplitude expression is determined as [12]

$$Y(\omega) = \frac{\Omega_0 \cdot X_0}{(\omega_{\text{sense}} - \omega_{\text{drive}})} \tag{2}$$

where ω_{sense} is the sense mode resonance frequency in rad/s. Compared with (1), (2) does not contain the improvement factor of Q_{sense}, and therefore, vacuum operation is not that critical for a gyroscope with slightly mismatched resonance frequencies. For the fabricated SYMDEC gyroscope, the drive and sense mode resonance frequencies are slightly mismatched due to

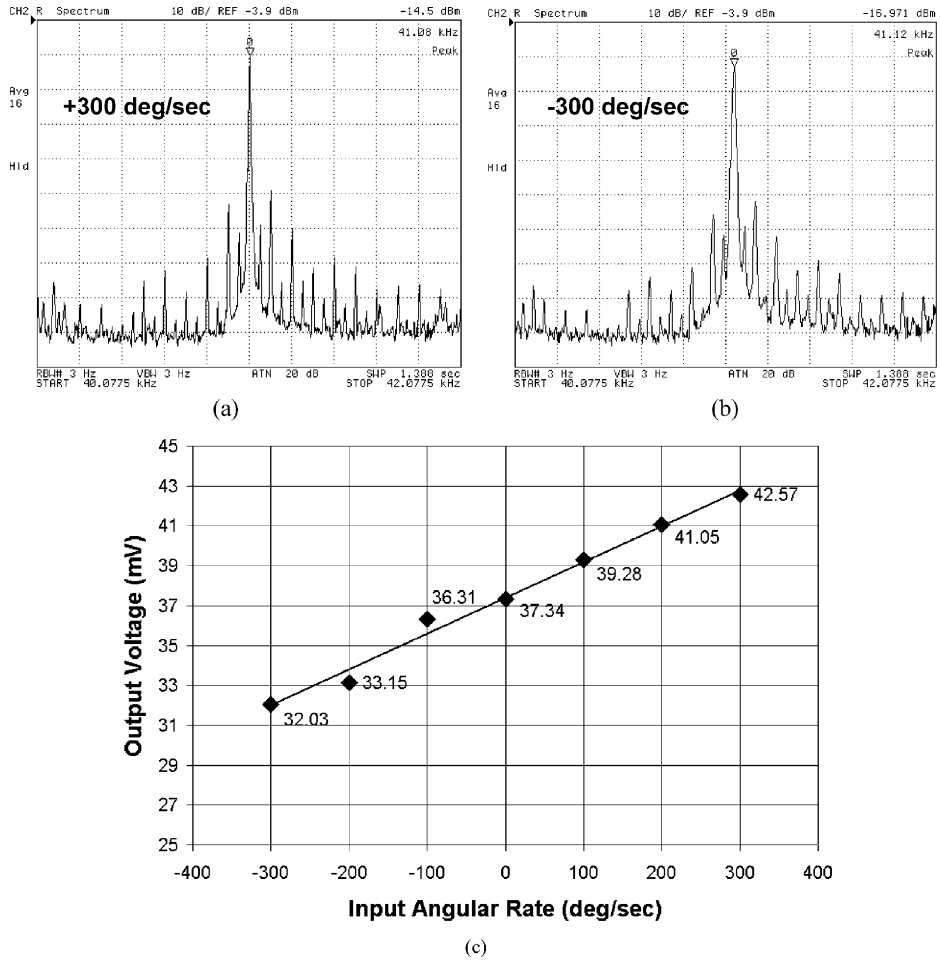

Fig. 17. Gyroscope output response for an angular rate inputs: (a) of $+300\ \mathrm{deg/s}$; (b) of $-300\ \mathrm{deg/s}$; and (c) from $-300\ \mathrm{deg/s}$ to $+300\ \mathrm{deg/s}$ with 100 deg/s steps. (a) and (b) show the spectrum analyzer outputs, whereas (c) shows the measurement results on a plot where the nonlinearity of the gyroscope response is determined to be less than 0.5%.

manufacturing tolerances. This mismatch can be removed by using additional electrostatic balance electrodes, which is under consideration for future designs. With the current design, the rate-sensitivity measurements are performed in the slight mismatched-mode operation. These results can be used to estimate the performance of the matched-mode operation.

The following analysis is carried out for the slightly mismatched case to verify that the predicted and measured results are consistent for the fabricated gyroscope. The gyro drive mode vibration amplitude is kept lower than 2 $\mu\mathrm{m}$ for both measurement and analysis to safely neglect nonlinear spring effects. The sense mode response of the gyro for this drive mode vibration amplitude is calculated to be 0.095 Angstroms for 1 deg/s angular rate input using (2) and the measured drive and sense mode resonance frequencies of 40 650 and 41 250 Hz, respectively. This amount of sense mode vibration corresponds to a capacitance change of 0.47 aF at the sense port, which yields an output voltage of 16 $\mu\mathrm{V}$ with the designed capacitive interface circuit that is fabricated in a commercial 0.8 $\mu\mathrm{m}$ CMOS foundry process. The output noise level of the readout circuit alone is measured as 1 $\mu\mathrm{V}$ in 1-Hz bandwidth, including direct electrical feedthrough from the parasitic capacitances due to wirebonding. As a result, the minimum detectable rate of the fabricated gyroscope is estimated to be about 0.45 deg/s in 50 Hz bandwidth. This value is verified by performing measurements on the fabricated gyroscopes using a rate table (Ideal Aerosmith, Inc.) with angular rate inputs from $-300\ \mathrm{deg/s}$ up to 300 deg/s. Fig. 16 shows the schematic of the test setup for measuring the angular rate response of the gyroscope. Fig. 17 shows the measured output response of the gyroscope for different angular rate inputs. The gyro output changes from 32 to 43 mV in that input range with a nonlinearity of only 0.5%, which corresponds to a scale factor of 17.6 $\mu\mathrm{V}/(\mathrm{deg/s})$ for the current SYMDEC gyroscope. The measured scale-factor is slightly higher than the expected scale factor due to electrostatic fringe-fields. The noise level of the hybrid system is measured as 2.4 $\mu\mathrm{V}$ in 3 Hz measurement bandwidth, which corresponds to an overall noise floor of 1.39 $\mu\mathrm{V}/\mathrm{Hz}^{1/2}$. Using these measured values, the rate resolution of the gyro is determined as 0.56 deg/s in a 50-Hz bandwidth, slightly higher than the expected value due to extra noise coming from the measurement setup. Excessive signal coupling is observed from the drive port to the sense port of the gyroscope through the parasitic capacitances associated with the measurement setup, which is measured to be about 35 mV. The amount of this coupling can be prevented by constructing the measurement setup on a PCB or SMD board. Excluding this

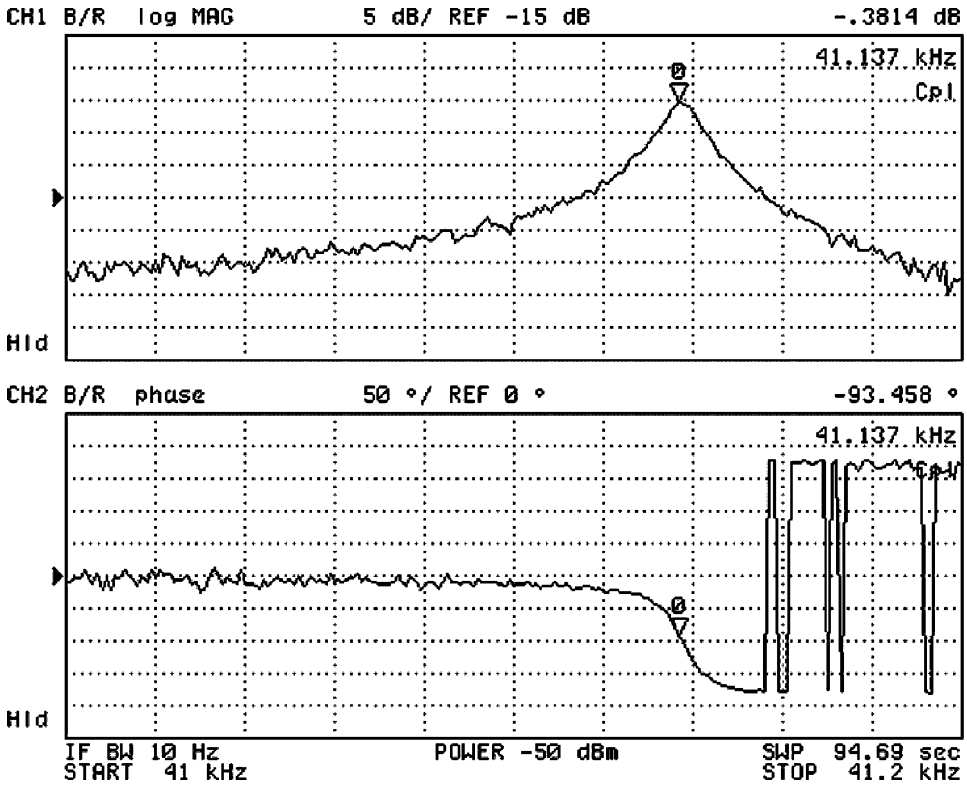

Fig. 18. Sense mode resonance response under 50 mtorr vacuum for the fabricated SYMDEC gyroscope, where the quality factor exceeds 14 000.

this coupling from the measured gyro output at zero rate input, the gyro bias is found to be about 2.5 mV. This value corresponds to 142 deg/s, which is in agreement with the simulated zero-rate output of 105 deg/s for single-ended scheme. Note that this bias value can be suppressed by using a differential sensing scheme, which is possible if a differential readout circuit is used.

The results of the angular rate measurements for the mismatched drive and sense mode resonance frequencies can be safely extended to estimate the gyro rate sensitivity for matched mode operation. The measured quality factors for the sense mode resonance at atmospheric pressure yields a minimum detectable rate of 0.030 deg/s for the current gyroscope in a bandwidth of 50 Hz with closed-loop operation, using the measured transfer function from the gyro output to the capacitive interface output and (1). This performance can be achieved without operating the gyroscope in vacuum environment, since the sense mode quality factor and hence the sense mode damping factor is already kept constant at a certain value by means of a feedback control loop.

Vacuum operation is important for applications where the input angular rate varies slowly in time. These applications generally require smaller bandwidths, but higher rate sensitivity. In these cases, the ultimate rate sensitivity for matched-mode operation of the proposed gyroscope is determined by the overall quality factor of the gyroscope. The effect of air damping on the overall quality factor can be neglected under vacuum conditions, where the mechanical dissipative mechanisms dominate. Fig. 18 shows the sense mode resonance response under 50 mTorr vacuum for the fabricated SYMDEC gyroscope. The peak displacement of the gyroscope at resonance is about 1.8 μm. The gyroscope demonstrates a quality factor of over 14 000 at vacuum. This quality factor would yield rate resolutions of 15 deg/h in a bandwidth of 3 Hz with open-loop operation and 0.017 deg/s in a bandwidth of 50 Hz with closed-loop operation. These rate resolution values are limited by the Brownian noise, and they can be improved further by using fabrication processes that allow thicker structural layers. Table I provides a summary of the performance specifications for the fabricated gyroscope structure.

TABLE I
SUMMARY OF THE PERFORMANCE SPECIFICATIONS FOR THE FABRICATED GYROSCOPE STRUCTURE

Specification	Value
Gyroscope size (mm^2)	1
Structural layer thickness (μm)	10
Drive mode resonance frequency (Hz)	40,650
Sense mode resonance frequency (Hz)	41,250
Sense gap (μm)	1.5
Sense capacitance (fF)	130
Polarization voltage (V)	40
Drive-mode vibration amplitude (μm)	2
Quality factor (atmospheric pressure)	500
Quality factor (50mTorr Vacuum)	14,000
Measurement range (deg/sec)	±300
Scale factor (μV/(deg/sec))	17,6
Non-linearity (%)	0.5
Readout cct. Noise ($\mu V/Hz^{1/2}$)	1.39
Minimum detectable rate (deg/sec)	0.56

VI. Conclusions and Future Work

This paper presents a single-crystal silicon symmetrical and decoupled microgyroscope implemented using the dissolved

wafer process on an insulating substrate. The symmetric structure allows matched resonant frequencies for the drive and sense vibration modes for high rate sensitivity and low temperature-dependent drift, while the decoupled drive and sense modes prevents unstable operation due to mechanical coupling, providing a low bias-drift. The gyroscope operation is verified by lumped element, finite element, and behavioral simulation tools, such as SPICE, CoventorWare, and SIMULINK. The measured electrode capacitances, resonance frequencies, and the rate sensitivities are found to be close to the simulated results based on the accurately constructed models. The 12–15 μm-thick single-crystal silicon structural layer with an aspect ratio of about 10 using DRIE patterning provides a high sense capacitance of 130 fF, while the insulating substrate provides a low parasitic capacitance of only 20 fF. The fabricated gyroscope is hybrid connected to a capacitive interface circuit fabricated in a 0.8-μm CMOS process and having a sensitivity of 34 mV/fF. Drive and sense mode resonance frequencies of the gyroscope are measured to be 40.65 and 41.25 kHz, respectively. Initial measurements show a rate resolution of 0.56 deg/s with slightly mismatched modes, which reveal that the gyroscope can provide a rate resolution of 0.030 deg/s in 50 Hz bandwidth with matched modes at atmospheric pressure. The gyroscope can also provide an ultimate rate resolution of 0.017 deg/s in 50-Hz bandwidth with closed-loop operation, limited by the thermomechanical noise when operated in 50-mtorr vacuum ambient. These rate resolution values can be improved even further by using fabrication processes that allow thicker structural layers. Such fabrication processes are currently under consideration along with gyroscope structures with electrostatic balance and control electrodes for matched-mode operation to obtain higher performance gyroscopes that can be used for many tactical-grade applications.

ACKNOWLEDGMENT

Authors would like to thank Dr. J. Chae and Prof. K. Najafi from The University of Michigan for their help with DRIE.

REFERENCES

[1] N. Yazdi, F. Ayazi, and K. Najafi, "Micromachined inertial sensors," *Proc. IEEE*, vol. 86, no. 8, pp. 1640–1659, Aug. 1998.

[2] Y. Mochida, M. Tamura, and K. Ohwada, "A micromachined vibrating rate gyroscope with independent beams for the drive and detection modes," in *Proc. 11th Int. Conf. Microelectromechanical Systems (MEMS'99)*, Orlando, FL, 1999, pp. 618–623.

[3] W. Geiger, J. Merz, T. Fischer, B. Folkmer, H. Sandmaier, and W. Lang, "The silicon angular rate sensors system MARS-RR," in *Proc. 10th Int. Conf. Solid-State Sens. Actuators (Transducers'99)*, Sendai, Japan, 1999, pp. 1578–1581.

[4] S. E. Alper and T. Akin, "A symmetric surface micromachined gyroscope with decoupled oscillation modes," *Sens. Actuators A*, vol. 97–98C, pp. 347–358, Apr. 2002.

[5] ——, "A symmetrical and decoupled microgyroscope with electroforming process on insulating substrate," in *Proc. 16th Europ. Conf. Solid-State Transducers (Eurosensors'02)*, Prague, Czech Republic, 2002, pp. 814–817.

[6] ——, "A symmetrical and decoupled nickel microgyroscope on insulating substrate," in *Proc. 17th Europ. Conf. on Solid-State Transducers (Eurosensors'03)*, Guimaraes, Portugal, 2003, pp. 24–27.

[7] ——, "A symmetrical and decoupled nickel microgyroscope on insulating substrate," *Sens. Actuators A, Phys.*, vol. 115/2-3, pp. 336–350, Sep. 2004.

[8] M. S. Kranz and G. K. Fedder, "Micromechanical vibratory rate gyroscopes fabricated in conventional CMOS," in *1997 Symp. Gyro Tech.*, pp. 3.0–3.8.

[9] S. E. Alper and T. Akin, "A single-crystal silicon symmetrical and decoupled gyroscope on insulating substrate," in *Proc. 12th Int. Conf. Solid-State Sens. Actuators (Transducers'03)*, Boston, MA, 2003, pp. 1399–1402.

[10] Y. Gianchandani and K. Najafi, "A bulk silicon dissolved wafer process for microelectromechanical systems," *J. Microelectromech. Syst.*, vol. 1, no. 2, pp. 77–85, Jun. 1992.

[11] W. Yun, R. T. Howe, and P. R. Gray, "Surface micromachined, digitally force-balanced accelerometer with integrated CMOS detection circuitry," in *Tech. Dig. 5th IEEE Solid-State Sensor and Actuator Workshop*, Hilton Head Island, SC, Jun. 22–25, 1992, pp. 21–25.

[12] S. D. Senturia, *Microsystem Design*. Boston, MA: Kluwer Academic, 2001, pp. 561–604.

Said Emre Alper was born in Ankara, Turkey, in 1976. He received the B.S. and M.Sc. degrees in electrical and electronics engineering with high honors from Middle East Technical University (METU), Ankara, in 1998 and 2000, respectively. He is currently working toward the Ph.D. degree in electrical and electronics engineering at METU.

Since 1998, he has been working as a research assistant with the MEMS VLSI Research Group, Department of Electrical and Electronics Engineering, METU. His major research interests include capacitive inertial sensors, micromachined resonators and actuators, capacitive interface circuits, and microfabrication technologies.

Mr. Alper received the first prize award in the operational designs category of the "International Design Contest" organized by DATE and CMP in March 2001, for his symmetric and decoupled gyroscope design. He also received the third prize award in the international "3-D MEMS Design Challenge" organized by MEMGEN Corporation (currently Microfabrica), in June 2003, for his tactical-grade symmetrical and decoupled microgyroscope design among 132 MEMS designs from 24 countries and 25 states across the U.S.

Tayfun Akin (S'90–M'97) was born in Van, Turkey, in 1966. He received the B.S. degree in electrical engineering with high honors from Middle East Technical University (METU), Ankara, Turkey, in 1987. He received a graduate fellowship provided by NATO Science Scholarship Program through the Scientific and Technical Research Council of Turkey (TUBITAK) in 1987. He received the M.S. degree and the Ph.D. degree in electrical engineering, both from the University of Michigan, Ann Arbor, in 1989 and 1994, respectively.

In 1995, 1998, and 2004, he was an Assistant Professor, Associate Professor, and Professor, respectively, in the Department of Electrical and Electronics Engineering, Middle East Technical University, Ankara. He is also the technical coordinator of METU-MET, an IC fabrication factory which is transferred to the METU by the government for MEMS-related production. His research interests include MEMS, microsystems technologies, infrared detectors and readout circuits, silicon-based integrated sensors and transducers, and analog and digital integrated circuit design.

Dr. Akin has served in various MEMS, EUROSENSORS, and TRANSDUCERS conferences as a Technical Program Committee Member. He is the designate co-chair of The 19th IEEE International Conference of Micro Electro Mechanical Systems (MEMS 2006) to be held in Istanbul. He is the winner of the First Prize in Experienced Analog/Digital Mixed-Signal Design Category at the 1994 Student VLSI Circuit Design Contest organized and sponsored by Mentor Graphics, Texas Instruments, Hewlett-Packard, Sun Microsystems, and Electronic Design Magazine. He is the coauthor of the symmetric and decoupled gyroscope project which won the first prize award in the operational designs category of the international design contest organized by DATE Conference and CMP in March 2001. He is also the coauthor of the gyroscope project which won the third prize award of 3-D MEMS Design Challenge organized by MEMGen Corporation (currently, Microfabrica).